Journal of Instrumentation

PAPER • **OPEN ACCESS**

Silicon microchannel frames for high-energy physics experiments

To cite this article: W. Poonsawat *et al* 2021 *JINST* **16** P08050

Jinst

Published by IOP Publishing for Sissa Medialab

Received: *December 3, 2020*
Accepted: *July 7, 2021*
Published: *August 17, 2021*

Silicon microchannel frames for high-energy physics experiments

W. Poonsawat,[a] J. Supadech,[b] N. Klunngien,[b] W. Jeamsaksiri,[b] N. Ritjoho,[c] N. Laojamnongwong,[c] A. Mapelli,[d] A. Francescon,[d] D. Alvarez Feito[d] and C. Kobdaj[c,*]

[a] *Department of Applied Physics, Rajamangala University of Technology Isan, 744 Suranarai Rd., Muang, Nakhon Ratchasima, 30000 Thailand*

[b] *Thai Microelectronics Center (TMEC), 51/4 Moo 1 Suwintawong Road, Wangtakien, Muang, Chachoengsao, 24000 Thailand*

[c] *School of Physics, Suranaree University of Technology, 111 University Avenue, Muang, Nakhon Ratchasima, 30000 Thailand*

[d] *Experimental Physics Department, CERN, CH-1211 Geneva 23, Switzerland*

E-mail: kobdaj@g.sut.ac.th

Abstract: The design of detectors used for experiments in high-energy physics requires a light, stiff, and efficient cooling system with a low material budget. The use of silicon microchannel cooling plates has gained considerable interest in the last decade. In this study, we propose the development of silicon microchannel cooling frames studied within the framework of the major upgrade of the Inner Tracking System (ITS) of the ALICE experiment at CERN. The preliminary results obtained with these frames demonstrate that they can withstand the internal pressure arising from the flow of the coolant with a limited mass penalty.

Keywords: Detector cooling and thermo-stabilization; Materials for solid-state detectors; Particle tracking detectors (Solid-state detectors)

*Corresponding author.

https://doi.org/10.1088/1748-0221/16/08/P08050

Contents

1 Introduction

Microchannel cooling exhibits excellent heat transfer properties and optimal integration characteristics. A microchannel cooling system is usually composed of a number of parallel channels of micrometer size where the cooling fluid runs through. This technology has raised considerable interest in the last decade for the thermal management of electronics devices [1]. Benefiting from the incredible progress of microfabrication technologies in recent years, microchannel cooling plates can be fabricated to feature microscopic parallel channels in very thin and light substrates. For these reasons, microchannel cooling has recently started to be considered for the thermal management of particle detectors in high energy physics experiments [2].

The first application of microchannel cooling in high-energy physics experiments has been in the GigaTracker (GTK) of the NA62 experiment [3] where silicon microchannel cooling plates are used to remove the heat dissipated locally by the electronic devices of the 60×40 mm^2 GTK modules, while maintaining the sensor temperature at below 0°C [4, 5]. This technology was later adopted for the Large Hadron Collider beauty experiment (LHCb) vertex locator (VeLo) upgrade [6]. It has also been extensively studied for the LS2 Upgrade of the ALICE inner tracking system (ITS) [7, 8]. Very strict requirements in terms of material budget contribution and high temperature uniformity for the ALICE ITS [9] have required a deep study that was conducted by the ALICE ITS community in close collaboration with CERN, the Suranaree University of Technology (SUT), Thai Microelectronics Center (TMEC), and École Polytechnique Fédérale de Lausanne (EPFL). In this study, we describe the fabrication processes and pressure tests of the microchannel prototypes.

2 Microfabrication technologies

Microfabrication technologies comprise a wide variety of techniques used for manufacturing microdevices. They are used to build microelectromechanical systems (MEMS) and microfluidic devices for miniature cooling systems. A microfabrication process flow is usually a sequence of various fabrication steps. The standard steps in microfabrication processing are photolithography, thin film deposition or structuration, etching, thinning by grinding or chemical mechanical polishing (CMP), bonding at wafer level or chip level, and dicing.

For the realization of silicon microfluidic cooling plates, microchannels are usually etched into silicon wafers and then sealed by bonding with another wafer, typically of silicon or glass. The etching process is performed either in a dry phase, typically with plasma, or in a wet phase. Plasma anisotropic etching results in vertical or near-vertical sidewalls independent of the crystalline orientation of the silicon wafers. Wet etching in a solution of potassium hydroxide (KOH) can lead to sloped sidewalls based on the crystalline orientation of the wafer. Indeed, KOH etch rates between different crystal planes differ by a factor of up to 200, thereby resulting in sloped sidewalls following the crystalline planes with the slowest etch rates.

To seal the cooling microchannels, two types of bonding are mostly employed. The first technique is anodic bonding between a structured silicon wafer and an unstructured Pyrex wafer (see figure 1(a)). The second is direct bonding between two silicon wafers (see figure 1(b)). On the one hand, the former technique is simpler to perform and less demanding in terms of surface preparation, but it must be performed between two different materials. On the other hand, direct bonding between two silicon wafers, e.g. a silicon fusion bonding technique, is very demanding in terms of surface quality but results in a very strong chemical bond. The microchannel device with fusion bonding technique shows higher durability than the device closing with Pyrex due to the better mechanical properties of monocrystalline silicon compared to borosilicate or Pyrex. Owing to very stringent requirements in terms of safety and reliability in the design of particle detectors in high-energy physics experiments, the latter technique is more suitable for application in this work.

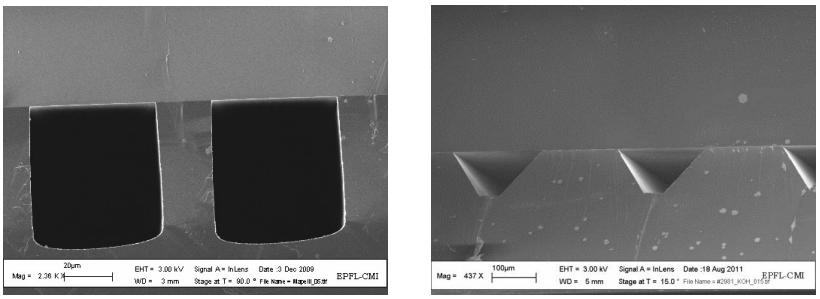

(a) (b)

Figure 1. Examples of silicon microchannel with different bonding techniques, (a) plasma etching (DRIE) closing by Pyrex, (b) wet etching (KOH solution) closing by a silicon wafer [10].

Microfluidic cooling devices investigated at CERN to remove the heat dissipated by the front-end electronics of silicon tracking detectors are fabricated with various process flows, thereby allowing each type of device to optimize their pressure limits. The fabrication proceeded in three

steps: etching of microchannels in silicon wafers, bonding of unstructured silicon wafers to close the microchannels, and thinning of the assembled cooling plates in the acceptance of the detectors.

3 Single-microchannel sample

To characterize the pressure resistance of microchannel cooling devices, samples of a single microchannel were fabricated and subjected to hydrostatic testing to failure.

3.1 Preparation

Single microchannel samples for pressure testing were fabricated in 4 inches silicon wafers with a thickness of 0.6 mm. All channels had the same length $L = 5$ mm and depth $D = 0.25$ mm. However, they had different widths of 0.2 mm, 0.35 mm, 0.5 mm, 0.7 mm, 1.0 mm, 1.2 mm, 1.25 mm, and 1.5 mm as shown in figure 2. A hole with a diameter of 1.6 mm allowed the fluid to be injected in the dead-end microchannel through a 0.05 mm wide capillary. The etched wafer with the single-microchannel was covered and bonded to another blank wafer. Subsequently, the bonded wafers were diced into samples with a footprint of 10×20 mm.

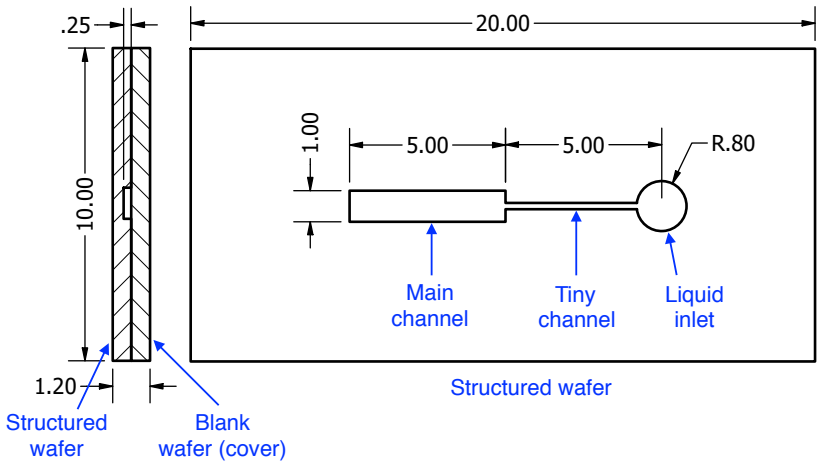

Figure 2. Geometry of the single-microchannel sample (all units in mm). The left and right pictures show the cross-section and top view of the sample respectively.

3.2 Pressure test procedures and results

The pressure tests of the single-microchannel samples have been performed at CERN. The testing device consisted of a water tank, a manual water pump with a maximum pressure of 700 bar, a sample holder, a pressure sensor, and a data acquisition system. The sample holder comprises a sample alignment tool and a fluid connector.

The single microchannel sample was placed in the sample holder and connected to the fluid connector. Water was then injected into the sample with a slightly increasing pressure until failure of the sample. This pressure was then marked as the pressure at the fracture. Test results are shown in figure 3 as the pressure at the rupture as a function of the microchannel width. As expected, the

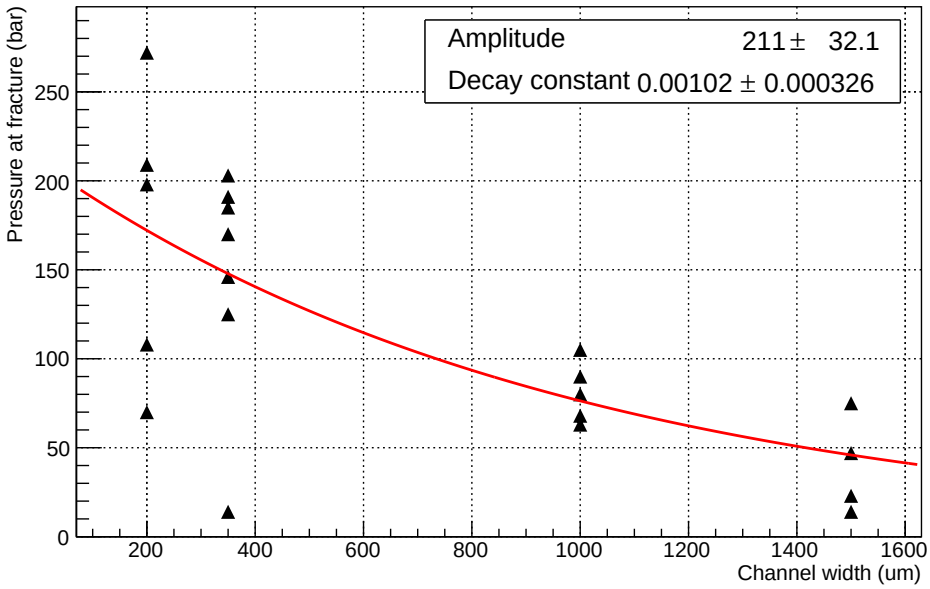

Figure 3. The pressure test results demonstrating the pressure at the fracture as a function of channel width.

pressure at the fracture decreases with the larger width of the channel, because for the larger width samples, the area exposed to the pressure or higher force acting on silicon surface is larger. The maximum pressure at the fracture is approximately 270 bar, as recorded by the sample with a width of 200 µm. These results show the upper limit (> 250 bar) of the pressure at fracture of our fabricated microchannel device that higher than the maximum required pressure of the inlet coolant at 10 bar.

The analysis of the samples after failure shows that the failure occurs at the bonding interface, meaning that the bonding method needs to be improved. From figure 3, the pressure at the failure for the sample with the smaller channel width (200 and 350 µm) broadly varies between 10–280 bar, whereas that for the sample with larger width (1000 and 1500 µm) demonstrates narrower variation about 10 to 100 bar. These huge variations from all of the samples with different channel widths demonstrate the instability of our poor bonding samples.

4 Multi-microchannels cooling device

4.1 Design of the multi-microchannel

The microchannel cooling system has a significantly smaller scale than the typical pipe cooling system, and this results in a considerably lower material budget. When a particle travels to a detector that consists of a low material budget, there is a lower possibility that the particle will scatter or change its energy. This can help increase detection efficiency and minimize the detection uncertainty of the detector owing to the lower possibility of particle scattering.

The microchannel cooling frames presented in this paper were fabricated from a 600 µm thick silicon wafer etched by dry processes, thereby resulting in microchannels with a depth of 100 µm and a 50 µm width of 63 mm lengths. Water or Freon with the saturated temperature of 15 °C is used

as a coolant. Its pressure changes depending on the temperature; it is liquid when it is compressed and becomes gas after heating. The microchannels are designed to have different lengths to observe the dependency of the microchannel length to the pressure durability.

A shorter microchannel reduces the likelihood of a phase transition in the coolant. This transition from liquid phase into gas phase increases its volume and indicates that the pressure dropped at the outlet. Therefore, it is expected to have higher strength. The finished microchannel plate was tested for pressure tolerance. The etched silicon wafer depicted in figure 4 is an initial structure used to study the durability of the wafer bonding process.

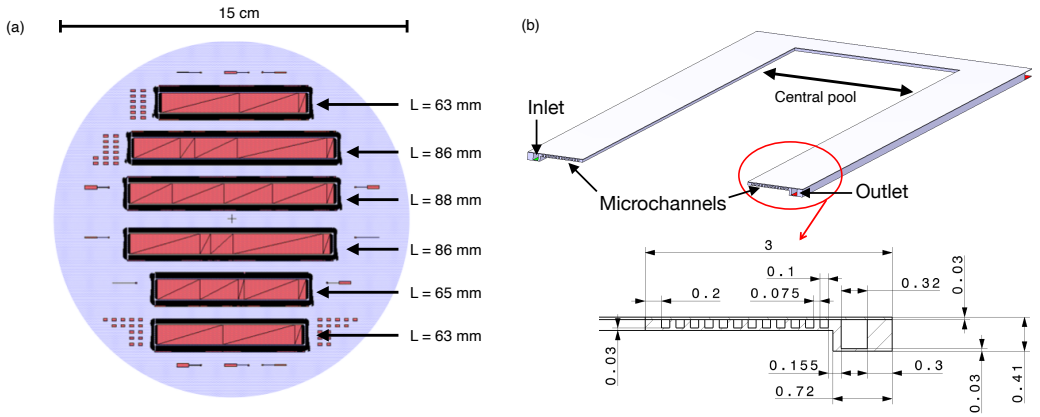

Figure 4. Design of the microchannel cooling system showing the dimension of (a) full-scale microchannel, (b) schematic layout of 12 channels and fluidic inlets.

4.2 Fabrication process of the multi-microchannel

Silicon multi-microchannel devices were fabricated in a cleanroom at the Thai Microelectronics Center (TMEC). The fabrication process is illustrated in figure 5.

The process started with cleaning 600 µm thick silicon wafers with the RCA process as a preparation step before lithography. After that (see figure 5(a)), layers of 1.5 µm silicon dioxide (SiO_2) were grown on both sides of the wafer by the wet oxidation method. To control the layer quality, the thickness of the SiO_2 was measured by an Ellipsometer. Then, 3.5 µm thickness of SiO_2 films were produced by the PECVD method on top of the previous layers. The method was performed in an atmosphere of SiH_4:N_2O=60:1200 at pressure 3.1 Torr, and 1050 °C. By these consequent methods, the wet oxidation method could confirm the denser nano-porous structure of the SiO_2 layer and the PECVD method could reduce the growing time of the film to reach the total 5 µm SiO_2 layer.

In the next step (see figure 5(b)), the photoresistor was patterning in the shape of the microchannel and central pool on the front side of the wafer by photolithography. The photoresist was used as the etching mask during the shallower Si etching; then, the underlying oxide mask was used for deeper etching owing to higher etch selectivity toward the Si for the deep reactive ion etching process. The center pool refers to the middle area of the sample that needs to be removed, located between two arrays of the microchannels. The center pool width is 9 mm and its length is different

depending on the microchannel length for each sample. Subsequently, the SiO_2 layers of the 5.0 µm thickness were etched by plasma.

Then (see figure 5(c)), the photoresistor was removed by O_2 plasma and Piranha solution. We performed fiducial markers by photolithography at the rear side of the wafer by etching 3.5 µm of the PECVD SiO_2 layer and 1.5 µm of SiO_2 layer from the wet oxidation process and finally etching 3.0 µm of the silicon bulk. The fiducial markers were used as references for an alignment. In figure 5(c), the photoresistor was patterned to avoid etching in parts of the microchannel. This results in etching of silicon bulk in parts of the central pool and main channels with the depth of 250 µm. After that, the photoresistor was removed by O_2 plasma and etching process was performed again in parts of the microchannel, main channel, and central pool. Then (see figure 5(d)), the wafer was structured by plasma etching in the shape of two arrays of microchannels and inlet/outlet on both sides and the central pool in the middle. The SiO_2 layers were removed by BOE solution as the surface treatment process. A shape of the pure structure silicon wafer without any oxide layer is demonstrated in figure 5(e).

Thereafter (see figure 5(f)), the structured wafer was bonded by the Fusion bond technique by another silicon wafer that contained 1.5 µm thickness of SiO_2 films on both sides. Owing to the oxide layer growth on the Si surface, the hydrophilic bonding process will be executed. The bonding started with the cleaned Si wafer by the RCA cleaning steps to remove the organic and ionic contamination with the chemical solution. Then, the wafers pass a dry-cleaning step, an O_2 plasma activation for 2 mins to get the hydroxyl group on the surface. After that, the cleaned surfaces of both Si are placed in close vicinity to generate the hydrogen bonds, called pre-bonding, at 200 °C and 6 kN. Finally, the contracted wafers are annealed up to 1040 °C for 2 hours to enhance the high strength bond. Again (see figure 5(g)), we performed fiducial markers on top of the second wafer. The photoresist was patterned on the top wafer to deeply etch the central pool. Moreover (see figure 5(h)), the photoresist was also patterned on the structured wafer to etch the unnecessary silicon material. The central pool was removed by a tweezer.

Next (see figure 5(i)), plasma etching was performed on the structured wafer again to make the inlet/out holes. In the last step, the bonded wafer was thinned, resulting in the wanted multi-microchannel cooling device. For the grinding process, firstly the inlet and outlet of the bonded wafer were closed by a UV tape to avoid any liquid flowing into the channels. The grinding wheel polished the cover wafer to thin the wafer from 600 µm into 100 µm. After that, the CMP technique was used to thin the grinded wafer from a thickness of 100 µm to only 30 µm. The fluid connector was done after separation of the microchannel by dicing.

5 Conclusions

Silicon microchannel cooling frames have been studied mechanically by high-pressure fluids within the framework of the LS2 upgrade of the ALICE ITS. The microchannel can be integrated with the silicon tracking detectors to dissipate the heat generated by the monolithic sensor. The high thermal conductivity of the microchannel ensures the required cooling efficiency, while maintaining minimal material budget [11]. TMEC demonstrated that the microfabrication process could allow the production of microchannel cooling devices with different channel widths. Nevertheless, the direct bonding of silicon wafers still requires further investigation.

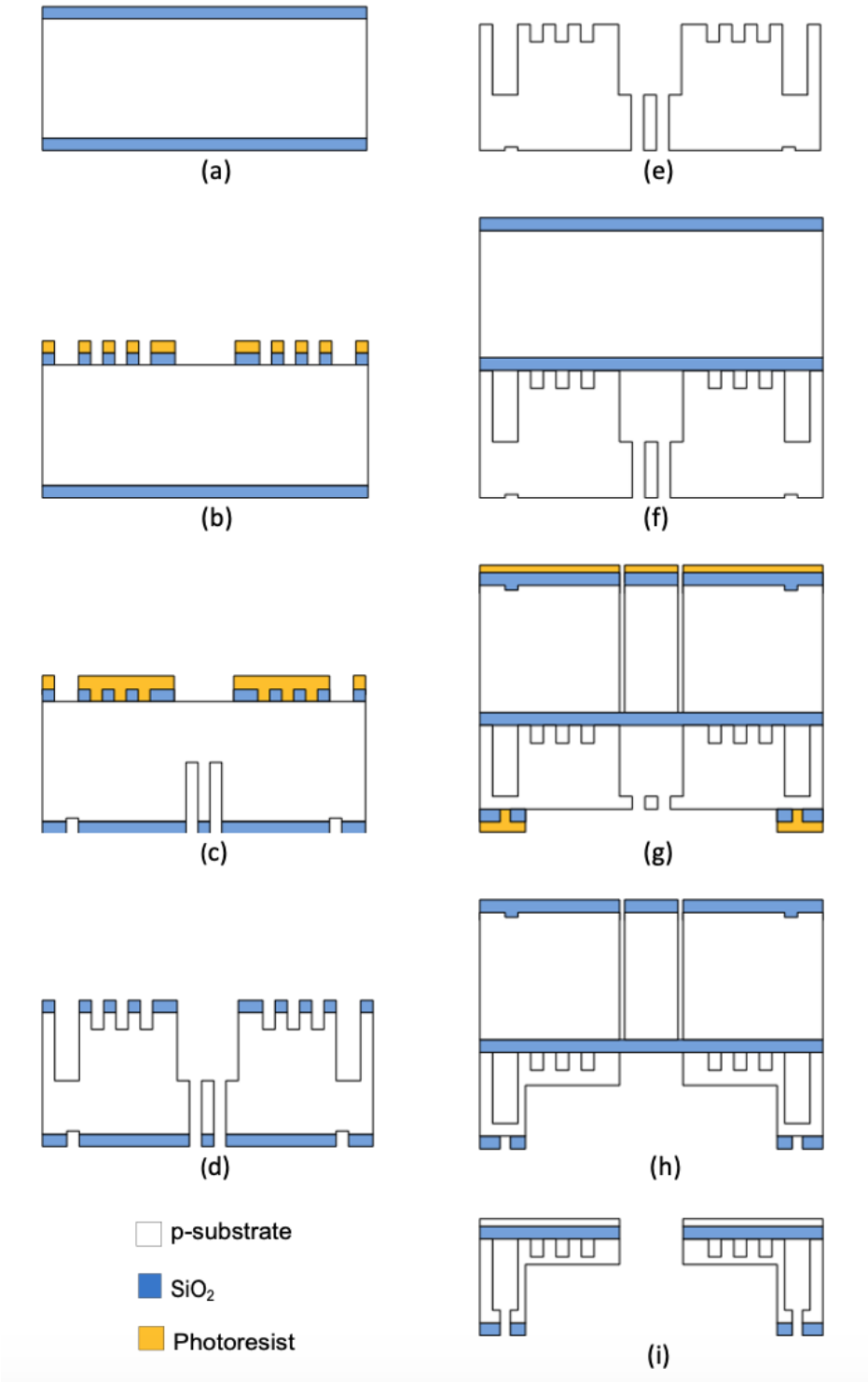

Figure 5. Simplified processes of microfabrication. (a) SiO_2 thin film deposition on both sides of the p-substrate, (b) patterning on the front side by photoresistor and etching by plasma, (c) patterning on the frontside by photoresistor and etching on the backside, (d) removal of the photoresistor, (e) removal of the deposited SiO_2, (f) closing etched wafer with another SiO_2 deposited wafer, (g) etching central pool, (h) removal of photoresistor, and (i) inlet and outlet etched with plasma.

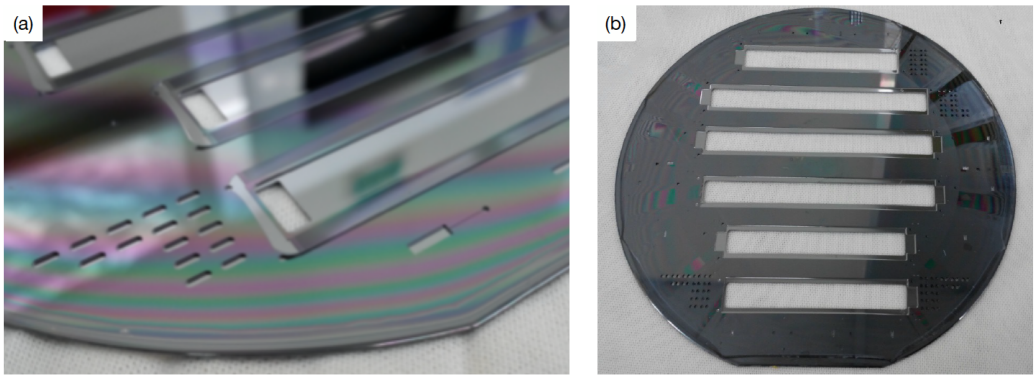

Figure 6. (a) The close-up picture of the silicon wafer showing the microchannels. (b) The structured silicon wafer after the removal of the central pools.

Starting with a single-microchannel construction, we demonstrated their resistance to high hydrostatic pressures. These results indicated that the pressure at the fracture is reduced by increasing the channel width. The prototype of the multi-microchannel device was fabricated by TMEC (see figure 6), and it was bonded by PHILIPS Innovation Services and sent to CERN for dicing and grinding. Such devices require further pressure tests.

The prototype of the microchannel cooling devices aims to preserve the distribution of the high-pressure refrigerant inside the structure. This concept is currently under development to improve the efficiency of thermal extraction for future HEP experiments.

Acknowledgments

We would like to thank Luciano Musa for useful discussions and Christoph Herold for commenting on the manuscript. We acknowledge the help and experimental support from the Thai Microelectronics Center (TMEC) for their efforts in demonstrating the microscale fabrication. This work was supported by Suranaree University of Technology (SUT), CHE-RNU project (SUT-COE: High Energy Physics & Astrophysics), Thailand Center of Excellence in Physics (ThEP), Thailand Science Research and Innovation (TSRI), and the National Science and Technology Development Agency (NSTDA-P-15-50416). TMEC is supported by the NSTDA-CPMO grant no. P-15-50617. Narongrit Ritjoho is supported by SUT-Postdoc Full-time61/18/2563.

References

[1] A. Mapelli, P. Petagna and P. Renaud, *Micro-channel cooling for high-energy physics particle detectors and electronics*, in proceedings of the *13th InterSociety Conference on Thermal and Thermomechanical Phenomena in Electronic Systems*, San Diego, CA, U.S.A., 30 May–1 June 2012, pp. 677–683.

[2] A. Mapelli, *Microfabricated silicon substrates for pixel detectors assembly and thermal management a.k.a. silicon microchannel cooling plates*, *Nucl. Instrum. Meth. A* **958** (2020) 162142.

[3] L. Federici et al., *The Gigatracker, the silicon beam tracker for the NA62 experiment at CERN*, *Nucl. Instrum. Meth. A* **958** (2020) 162127.

[4] L. Federici et al., *The Gigatracker detector of the NA62 experiment at CERN SPS*, *Nucl. Instrum. Meth. A* **936** (2019) 715.

[5] G. Aglieri Rinella et al., *The NA62 GigaTracKer: a low mass high intensity beam 4D tracker with 65 ps time resolution on tracks*, 2019 *JINST* **14** P07010 [arXiv:1904.12837].

[6] LHCb VELO, VELO Upgrade collaboration, *The LHCb VELO (VErtex LOcator) and the LHCb VELO upgrade*, *Nucl. Instrum. Meth. A* **699** (2013) 160.

[7] ALICE collaboration, *Technical Design Report for the Upgrade of the ALICE Inner Tracking System*, *J. Phys. G* **41** (2014) 087002.

[8] A. Mapelli, *Low mass integrated cooling*, *PoS* **Vertex2013** (2013) 046.

[9] A. Francescon, G. Romagnoli, A. Mapelli, P. Petagna, C. Gargiulo, L. Musa et al., *Development of interconnected silicon micro-evaporators for the on-detector electronics cooling of the future ITS detector in the ALICE experiment at LHC*, *Appl. Therm. Eng.* **93** (2016) 1367.

[10] A. Mapelli, P. Petagna, K. Howell, G. Nuessle and P. Renaud, *Microfluidic cooling for detectors and electronics*, 2012 *JINST* **7** C01111.

[11] ALICE ITS collaboration, *Stave module design and development of the new ALICE Inner Tracking System*, 2019 *JINST* **14** P05003.